Nitrate-driven urban haze pollution during summertime over the North China Plain

Haiyan Li[1], Qiang Zhang[2], Bo Zheng[3], Chunrong Chen[2], Nana Wu[2], Hongyu Guo[4], Yuxuan Zhang[2], Yixuan Zheng[2], Xin Li[2], Kebin He[1,5]

[1] State Key Joint Laboratory of Environment Simulation and Pollution Control, School of Environment, Tsinghua University, Beijing 100084, China

[2] Ministry of Education Key Laboratory for Earth System Modeling, Department of Earth System Science, Tsinghua University, Beijing 100084, China

[3] Laboratoire des Sciences du Climat et de l'Environnement, CEA-CNRS-UVSQ, UMR8212, Gif-sur-Yvette, France

[4] School of Earth and Atmospheric Sciences, Georgia Institute of Technology, Atlanta, GA, 30332, USA

[5] State Environmental Protection Key Laboratory of Sources and Control of Air Pollution Complex, Tsinghua University, Beijing 100084, China

Correspondence to: Qiang Zhang (qiangzhang@tsinghua.edu.cn) or Kebin He (hekb@tsinghua.edu.cn)

Abstract. Compared to the severe winter haze episodes in the North China Plain (NCP), haze pollution during summertime has drawn little public attention. In this study, we present the highly time-resolved chemical composition of submicron particles (PM_1) measured in Beijing and Xinxiang in the NCP region during summertime to evaluate the driving factors of aerosol pollution. During the campaign periods (30 June to 27 July, 2015, for Beijing and 8 to 25 June, 2017, for Xinxiang), the average PM_1 concentrations were 35.0 μg m^{-3} and 64.2 μg m^{-3} in Beijing and Xinxiang, respectively. Pollution episodes characterized with largely enhanced nitrate concentrations were observed at both sites. In contrast to the slightly decreased mass fractions of sulfate, semi-volatile oxygenated organic aerosol (SV-OOA), and low-volatile oxygenated organic aerosol (LV-OOA) in PM_1, nitrate displayed a significantly enhanced contribution with the aggravation of aerosol pollution, highlighting the importance of nitrate formation as the driving force of haze evolution in summer. Rapid nitrate production mainly occurred after midnight, with a higher formation rate than that of sulfate, SV-OOA, or LV-OOA. Based on observation measurements and thermodynamic modeling, high ammonia emissions in the NCP region favored the high nitrate production in summer. Nighttime nitrate formation through heterogeneous hydrolysis of dinitrogen pentoxide (N_2O_5) enhanced with the development of haze pollution. In addition, air masses from surrounding polluted areas during haze episodes also led to more nitrate production. Finally, atmospheric particulate nitrate data acquired by mass spectrometric techniques from various field campaigns in Asia, Europe, and North America uncovered a higher concentration and higher fraction of nitrate present in China. Although measurements in Beijing during different years demonstrate a decline in the nitrate concentration in recent years, the nitrate contribution in PM_1 still remains high. To effectively alleviate particulate matter pollution in summer, our results call for the urgent need to initiate ammonia emission control measures and further reduce nitrogen oxide emissions over the NCP region.

1 Introduction

Atmospheric aerosol particles are known to significantly impact visibility (Watson, 2002) and human health (Pope et al., 2009; Cohen et al., 2017), as well as affect climate change by directly and indirectly altering the radiative balance of Earth's atmosphere (IPCC, 2007). The effects of aerosols are intrinsically linked to the chemical composition of particles, which are usually dominated by organics and secondary inorganic aerosols (i.e., sulfate, nitrate, and ammonium) (Jimenez et al., 2009).

In recent years, severe haze pollution has repeatedly struck the North China Plain (NCP), and its effects on human health have drawn increasing public attention. Correspondingly, the chemical composition, sources, and evolution processes of particulate

matter (PM) have been thoroughly investigated (Huang et al., 2014; Guo et al., 2014; Cheng et al., 2016; Li et al., 2017a), mostly during extreme pollution episodes in winter. Unfavorable meteorological conditions, intense primary emissions from coal combustion and biomass burning, and fast production of sulfate through heterogeneous reactions were found to be the driving factors of heavy PM accumulation in the NCP region (Zheng et al., 2015; Li et al., 2017b; Zou et al., 2017). Although summer is characterized by relatively better air quality compared to the serious haze pollution in winter, fine particle ($PM_{2.5}$) concentration in the NCP region still remains high during summertime. Through one-year real-time measurements of non-refractory submicron particles (NR-PM_1), Sun et al. (2015) showed that the aerosol pollution during summer was comparable to that during other seasons in Beijing, and the hourly maximum concentration of NR-PM_1 during the summer reached over 300 μg m^{-3}. Previous studies focusing on the seasonal variations of aerosol characteristics have noted quite different behaviors of aerosol species in winter and summer (Hu et al., 2017). Therefore, figuring out the specific driving factors of haze evolution in summer would help establish effective air pollution control measures.

Compared to more than 70% reduction of sulfur dioxide (SO_2) emissions since 2006 due to the wide application of flue-gas desulfurization devices in power plants and the phase-out of small, high emitting power generation units (Li et al., 2017c), nitrogen oxide (NO_x) emissions in China remain high and decreased by less than 20% from 2012 to 2015 (Liu et al., 2016). Therefore, the role of nitrate formation in aerosol pollution is predicted to generally increase as a consequence of high ammonia (NH_3) emissions in the NCP region. However, due to the significantly enhanced production of sulfate in extreme winter haze resulting from the high relative humidity (RH) and large SO_2 emissions from coal combustion, little attention has been paid to nitrate behaviors. In $PM_{2.5}$, aerosol nitrate mostly exists in the form of ammonium nitrate, via the neutralization of nitric acid (HNO_3) with NH_3. HNO_3 is overwhelmingly produced through secondary oxidation processes, NO_2 oxidized by OH during the day and hydrolysis of N_2O_5 at night, with the former being the dominant pathway (Alexander et al., 2009). The neutralization of HNO_3 is limited by the availability of NH_3, as NH_3 prefers to react first with sulfuric acid (H_2SO_4) to form ammonium sulfate with lower volatility (Seinfeld and Pandis, 2006). Because ammonium nitrate is semi-volatile, its formation also depends on the gas-to-particle equilibrium, which is closely related to variations in temperature and RH. A recent review on PM chemical characterization summarized that aerosol nitrate accounts for 16~35% of submicron particles (PM_1) in China (Li et al., 2017a). Some studies also pointed out the importance of aerosol nitrate in haze formation in the NCP region (Sun et al., 2012; Ge et al., 2017; Yang et al., 2017). However, detailed investigations and the possible mechanisms governing nitrate behaviors during pollution evolution are still very limited.

In this study, we present in-depth analysis of the chemical characteristics of PM_1 at urban sites in Beijing and Xinxiang, China during summertime. Based on the varying aerosol composition with the increase of PM_1 concentration, the driving factors of haze development were evaluated, and the significance of nitrate contribution was uncovered. In particular, we investigated the chemical behavior of nitrate in detail and revealed the factors favoring rapid nitrate formation during summer in the NCP region.

2 Experiments

2.1 Sampling site and instrumentation

The data presented in this study were collected in Beijing from 30 June to 27 July, 2015, and in Xinxiang from 8 to 25 June, 2017. Beijing is the capital city of China, adjacent to Tianjin municipality and Hebei province, both bearing high emissions of air pollutants. The Beijing-Tianjin-Hebei region is regularly listed as one of the most polluted areas in China by the China National Environmental Monitoring Centre. The field measurements in Beijing were performed on the roof of a three-floor building on the campus of Tsinghua University (40.0 °N, 116.3 °E). The sampling site is surrounded by school and residential areas, and no major

industrial sources are located nearby. Xinxiang is a prefecture-level city in northern Henan province, characterized by considerable industrial manufacturing. In February 2017, the Chinese Ministry of Environmental Protection issued the "Beijing-Tianjin-Hebei and the surrounding areas air pollution prevention and control work program 2017" to combat air pollution in Northern China. The action plan covers the municipalities of Beijing and Tianjin and 26 cities in Hebei, Shanxi, Shandong and Henan provinces, referred to as "2+26" cities. The 26 cities were identified according to their impacts on Beijing's air quality through regional air pollution transport. Xinxiang is listed as one of the "2+26" cities. The average $PM_{2.5}$ concentrations in Xinxiang in 2015 and 2016 were 94 μg m^{-3} and 84 μg m^{-3}, respectively. Our sampling in Xinxiang was performed in the mobile laboratory of Nanjing University, deployed in the urban district near an air quality monitoring site (35.3 °N, 113.9 °E). The observations in both Beijing and Xinxiang would help to figure out the generality and individuality of air pollution in the NCP region.

An Aerodyne Aerosol Chemical Speciation Monitor (ACSM) was deployed for the chemical characterization of NR-PM_1, with a time resolution of 15 minutes. Briefly, ambient aerosols were sampled into the ACSM system at a flow rate of 3 L min^{-1} through a $PM_{2.5}$ cyclone to remove coarse particles and then a silica gel diffusion dryer to keep particles dry (RH < 30%). After passing through a 100 μm critical orifice mounted at the entrance of an aerodynamic lens, aerosol particles with a vacuum aerodynamic diameter of ~30-1000 nm were directly transmitted into the detection chamber, where non-refractory particles were flash vaporized at the oven temperature (~600 °C) and chemically characterized by 70 eV electron impact quadrupole mass spectrometry. Detailed descriptions of the ACSM technique can be found in Ng et al. (2011). The mass concentration of refractory BC in PM_1 was recorded by a multi-angle absorption photometer (MAAP Model 5012, Thermo Electron Corporation) on a 10-min resolution basis (Petzold and Schönlinner, 2004; Petzold et al., 2005). The MAAP was equipped with a PM_1 cyclone, and a drying system was incorporated in front of the sampling line. A suite of commercial gas analyzers (Thermo Scientific) were also deployed to monitor variations in the gaseous species (i.e., CO, O_3, NO, NO_x, and SO_2).

For observations in Beijing, the total PM_1 mass was simultaneously measured using a PM-714 Monitor (Kimoto Electric Co., Ltd., Japan) based on the β-ray absorption method (Li et al., 2016). Meteorological conditions, including temperature, RH, wind speed, and wind direction, were reported by an automatic meteorological observation instrument (Milos520, VAISALA Inc., Finland). For measurements in Xinxiang, the online $PM_{2.5}$ mass concentration was measured using a heated Tapered Elemental Oscillating Microbalance (TEOM series 1400a, Thermo Scientific). The temperature and RH were obtained using a Kestrel 4500 Pocket Weather Tracker.

2.2 ACSM data analysis

The mass concentrations of aerosol species, including organics, sulfate, nitrate, ammonium, and chloride, can be determined from the ion signals detected by the quadrupole mass spectrometer (Ng et al., 2011) using the standard ACSM data analysis software (v.1.5.3.0) within Igor Pro (WaveMetrics, Inc., Oregon USA). Default relative ionization efficiency (RIE) values were assumed for organics (1.4), nitrate (1.1), and chloride (1.3). The RIEs of ammonium and sulfate were determined to be 7.16 and 1.08, respectively, through calibration with pure ammonium nitrate and ammonium sulfate. To account for the incomplete detection of aerosol particles (Ng et al., 2011), a constant collection efficiency (CE) of 0.5 was applied to the entire dataset. After all the corrections, the mass concentration of ACSM NR-PM_1 plus BC was closely correlated with that of total PM_1 obtained by PM-714 in Beijing (r^2 = 0.59; Fig. S1). The slope was slightly higher than 1, which was probably caused by different measuring methods of the different instruments and the uncertainties. For measurements in Xinxiang, the mass concentration of ACSM NR-PM_1 plus BC also displayed a good correlation with $PM_{2.5}$ concentration measured by TEOM, with a slope of 0.83 (r^2 = 0.85; Fig. S1).

Positive matrix factorization (PMF) with the PMF2.exe algorithm (Paatero and Tapper, 1994) was performed on ACSM organics mass spectra to explore various sources of organic aerosol (OA). Only *m/z*'s up to 120 were considered due to the higher

uncertainties of larger *m/z*'s and the interference of the naphthalene internal standard at *m/z* 127-129. In general, signals with *m/z* > 120 only account for a minor fraction of total signals. Therefore, this kind of treatment has little effect on the OA source apportionment. PMF analysis was performed with an Igor Pro-based PMF Evaluation Tool (PET) (Ulbrich et al., 2009), and the results were evaluated following the procedures detailed in Ulbrich et al. (2009) and Zhang et al. (2011). According to the interpretation of the mass spectra, the temporal and diurnal variations of each factor, and the correlation of OA factors with external tracer compounds, a four-factor solution with FPEAK = 0 and a three-factor solution with FPEAK = 0 were chosen as the optimum solutions in Beijing and Xinxiang, respectively. The total OA in Beijing was resolved into a hydrocarbon-like OA (HOA) factor, a cooking OA (COA) factor, a semi-volatile oxygenated OA (SV-OOA) factor, and a less-volatile oxygenated OA (LV-OOA) factor, where the former two represented primary sources, and the latter two came from secondary formation processes. In Xinxiang, the identified OA factors included HOA, SV-OOA, and LV-OOA. Procedures for OA source apportionment are detailed in the supplementary materials (Text S1; Tables S1-2; Figs. S2-7).

2.3 ISORROPIA-II equilibrium calculation

To investigate factors influencing the particulate nitrate formation, the ISORROPIA-II thermodynamic model was used to determine the equilibrium composition of an NH_4^+ - SO_4^{2-} - NO_3^- - Cl^- - Na^+ - Ca^{2+} - K^+ - Mg^{2+} - water inorganic aerosol (Fountoukis and Nenes, 2007). When applying ISORROPIA-II, we assumed that the aerosol was internally mixed and composed of a single aqueous phase, and the bulk PM_1 or $PM_{2.5}$ properties had no compositional dependence on particle size. The validity of the model performance for predicting particle pH, water, and semi-volatile species has been examined by a number of studies in various locations (Guo et al., 2015, 2016, 2017a; Hennigan et al., 2015; Bougiatioti et al., 2016; Weber et al., 2016; Liu et al., 2017). In this study, the sensitivity analysis of PM_1 nitrate formation to gas-phase NH_3 and PM_1 sulfate concentrations was performed using the ISORROPIA-II model, running in the "forward mode" for a metastable aerosol state. Input to ISORROPIA-II includes the average RH, T, and total NO_3^- (HNO_3 + NO_3^-) for typical summer conditions (RH = 56%, T = 300.21K) in Beijing and Xinxiang, along with a selected sulfate concentration. Total NH_4^+ (NH_3 + NH_4^+) was left as the free variable. The variations in nitrate partitioning ratio ($\varepsilon(NO_3^-) = NO_3^-/(HNO_3 + NO_3^-)$) were examined with varying sulfate concentrations from 0.1 to 45 μg m^{-3} and equilibrated NH_3 between 0.1 and 50 μg m^{-3}.

2.4 Air mass trajectory analysis

Back trajectory analysis using the Hybrid Single-Particle Lagrangian Integrated Trajectory (HYSPLIT) model (Draxler and Hess, 1998) was conducted to explore the influence of regional transport on aerosol characteristics in Beijing. The meteorological input was adopted from the NOAA Air Resource Laboratory Archived Global Data Assimilation System (GDAS) (ftp://arlftp.arlhq.noaa.gov/pub/archives/). The back trajectories initialized at 100 m above ground level were calculated every hour throughout the campaign and then clustered into several groups according to their similarity in spatial distribution. In this study, a four-cluster solution was adopted, as shown in Fig. S8.

3 Results and discussion

3.1 Overview of aerosol characteristics

Summer is usually the least polluted season of the year in the NCP region due to favorable weather conditions and lower emissions from anthropogenic sources (Hu et al., 2017). Figures 1 and 2 show the time series of meteorological parameters, gaseous species concentrations, and aerosol species concentrations in Beijing and Xinxiang. The weather during the two campaigns was relatively

hot (average T = 27.1 ± 4.1 ℃ for Beijing and 26.9 ± 4.0 ℃ for Xinxiang) and humid (average RH = 55.9 ± 18.5% for Beijing and 63.5 ± 17.2% for Xinxiang), with regular variations between day and night. The average PM_1 (= NR-PM_1 + BC) concentration was 35.0 μg m^{-3} in Beijing and 64.2 μg m^{-3} in Xinxiang, with the hourly maximum reaching 114.9 μg m^{-3} and 208.1 μg m^{-3}, respectively. Several pollution episodes were clearly observed at the two sites, along with largely increased nitrate concentrations. Secondary inorganic aerosol, including sulfate, nitrate, and ammonium, dominated the PM_1 mass with an average contribution above 50%. The higher nitrate fraction (24% in Beijing and 26% in Xinxiang) is similar to previous observations during summer (Sun et al., 2015; Hu et al., 2016), likely due to photochemical processes being more active than in winter. The mass fraction of OA is lower than that measured during winter in the NCP region (Hu et al., 2016; Li et al., 2017b), in accordance with the large reduction of primary emissions in summer. According to the source apportionment results, OA at both sites is largely composed of secondary factors, in which 44-52% is LV-OOA and 22-23% is SV-OOA (Figs. S4-5). Primary organic aerosol accounts for only 34% and 24% of the total OA in Beijing and Xinxiang, respectively. As there is no need for residential home-heating in summer, which results in lower air pollutant emissions from coal combustion, chloride accounts for a smaller fraction of approximately 1% in total PM_1.

The diurnal variations of aerosol species are similar in the measurements from Beijing and Xinxiang (Fig. S9). Organics demonstrated two pronounced peaks at noon and in the evening. Source characterization of OA suggested that the noon peak was primarily driven by cooking emissions, while the evening peak was a combination of various primary sources, i.e., traffic and cooking. Relatively flat diurnal cycles were observed for sulfate, suggesting that the daytime photochemical production of sulfate may be masked by the elevated boundary layer height after sunrise. Nitrate displayed lower concentrations in the afternoon and higher values at night.

3.2 Enhancement of nitrate formation during pollution episode

To effectively mitigate aerosol pollution through policy-making, the driving factors of the PM increase need to be determined. Figure 3 illustrates the mass contributions of various species in PM_1 as a function of PM_1 concentration in Beijing and Xinxiang. OA dominated PM_1 at lower mass loadings (> 40% when PM_1 < 20 μg m^{-3}), but its contribution significantly decreased with increased PM_1 concentration. The source apportionment of OA demonstrated that the large reduction in OA fraction was primarily driven by POA, especially in Beijing. The contribution of SV-OOA and LV-OOA decreased slightly as a result of the photochemical production. The results here are largely different from our winter study in Handan, a seriously polluted city in Northern China, where primary OA emissions from coal combustion and biomass burning facilitated haze formation (Li et al., 2017b). While in Beijing the contribution of sulfate increased slightly at lower PM_1 concentrations, the sulfate fraction generally presented a mild decrease with elevated PM_1 mass at the two sites. By contrast, nitrate displayed an almost linearly enhanced contribution with increased PM_1. Accordingly, the nitrate/sulfate mass ratio steadily increased as PM_1 went up.

Notably, the large enhancement of nitrate production mainly occurred after midnight. Figure 4 displays the scatter plots of nitrate versus PM_1 as well as sulfate versus PM_1 for comparison, both color-coded by the time of day. Though the ratios of sulfate versus PM_1 mostly increased in the afternoon, nitrate versus PM_1 showed steeper slopes from midnight to early morning. The correlation of nitrate with SV-OOA and LV-OOA also indicated that the formation rate of nitrate is considerably higher than that of SV-OOA and LV-OOA after midnight (Fig. S10). Therefore, we further checked the variations in the mass fractions of aerosol species as a function of PM_1 concentration for two periods, 0:00 to 11:00 and 12:00 to 23:00. Taking Beijing as an example, both the nitrate contribution in PM_1 and the nitrate/sulfate ratio were significantly enhanced for the period of 0:00 to 11:00 (Fig. S11). These results suggest that rapid nitrate formation is mainly associated with nighttime productions, when the heterogeneous hydrolysis of N_2O_5 dominates the formation pathways (Pathak et al., 2011). The observed high N_2O_5 concentrations in urban Beijing further support

our hypothesis (Wang et al., 2017). In addition, a recent study by Sun et al (2018) revealed that more ammonium nitrate content can reduce mutual deliquescence relative humidity (MDRH). With the enhanced formation of nitrate and higher RH during night, the heterogeneous reactions in the liquid surface of aerosols would result in more nitrate formation. Because the materiality of nitrate formation to haze evolution was observed in both Beijing and Xinxiang, we regard this as the regional generality in summer. Considering the efficient reduction in SO_2 emissions in China (Zhang et al., 2012), the results here highlight the necessity of further NO_x emission control for effective air pollution reduction in Northern China.

3.3 Factors influencing the rapid nitrate formation

Submicron nitrate mainly exists in the form of semi-volatile ammonium nitrate and is produced by the reaction of NH_3 with HNO_3 in the atmosphere. The formation pathways of HNO_3 include the oxidation of NO_2 by OH during the day and the hydrolysis of N_2O_5 at night. Thus, to investigate factors influencing the rapid nitrate formation in summer, the following conditions need to be considered: (1) the abundance of ammonia in the atmosphere, (2) the influence of temperature and RH, and (3) different daytime and nighttime formation mechanisms. Here, we explore nitrate formation processes based on Beijing measurements.

Under real atmospheric conditions, NH_3 tends to first react with H_2SO_4 to form $(NH_4)_2SO_4$ due to its stability (Seinfeld and Pandis, 2006). Thus, if possible, each mole of sulfate will remove 2 moles of NH_3 from the gas phase. NH_4NO_3 is formed when excess NH_3 is available. During the sampling period, the observed molar ratios of ammonium to sulfate were mostly larger than 2 (Fig. 5), corresponding to an excess of NH_3. The scatter plot of the molar concentration of excess ammonium versus the molar concentration of nitrate showed that, nitrate was completely neutralized by excess ammonium at most times. When ammonium is in deficit, nitrate may associate with other alkaline species or be part of an acidic aerosol (Kouimtzis and Samara, 1995).

Based on the ISORROPIA-II thermodynamic model, we performed a comprehensive sensitivity analysis of nitrate formation to the gas-phase NH_3 and PM_1 sulfate concentrations. Under typical Beijing summer conditions (T = 300.21K, RH = 56%), we assumed that total inorganic nitrate (HNO_3 + NO_3^-) in the atmosphere was 10 μg m^{-3}. Total ammonia (gas + particle) and PM_1 sulfate concentrations were independently varied and input in the ISORROPIA-II model. The predicted equilibrium of the nitrate partitioning ratio ($\varepsilon(NO_3^-) = NO_3^-/(HNO_3 + NO_3^-)$) is shown in Fig. 6. At a sulfate concentration from 0.1 to 45 μg m^{-3}, a 10 μg m^{-3} increase of gaseous NH_3 generally results in an enhancement of $\varepsilon(NO_3^-)$ by around 0.1 units or even higher, thus increasing the particulate nitrate concentration. The variations of gaseous NH_3 and $\varepsilon(NO_3^-)$ are not linearly related. Interestingly, for ammonia-rich systems, the existence of more particulate sulfate favors the partitioning of nitrate towards the particle phase. The formation of particulate ammonium nitrate is a reversible process with dissociation constant K_p:

$$NH_3(g) + HNO_3(g) \leftrightarrows NH_4NO_3(s) \quad (1)$$

K_p equals the product of the partial pressures of gaseous NH_3 and HNO_3. For an ammonium sulfate-nitrate solution, K_p not only depends on temperature and RH but also on sulfate concentrations, which is usually expressed by the parameter *Y* (Seinfeld and Pandis, 2006):

$$Y = \frac{[NH_4NO_3]}{[NH_4NO_3]+3[(NH_4)_2SO_4]} \quad (2)$$

When the concentration of ammonium sulfate increases compared to that of ammonium nitrate, the parameter Y decreases and the equilibrium product of NH_3 and HNO_3 decreases. The additional ammonium and sulfate ions make the system favorable for the heterogeneous formation of ammonium nitrate, by increasing particle liquid water content but not perturbing particle pH significantly. Particle pH is not highly sensitive to sulfate and associated ammonium (Weber et al., 2016; Guo et al., 2017b). Therefore, more ammonium sulfate in the aqueous solution will tend to increase the concentration of ammonium nitrate in the particle phase. As shown in Fig. 6, at a certain concentration of gaseous NH_3, the increase of sulfate concentration results in a

higher $\varepsilon(NO_3^-)$ and more particulate nitrate. Generally, these results suggest that the decreases in SO_2 emissions and NH_3 emissions are effective on nitrate reduction, indicating the importance of multi-pollutant control strategy in Northern China.

The influence of temperature and RH on nitrate formation was also evaluated based on ISORROPIA-II simulations by varying temperature and RH separately. As shown in Fig. S12, under typical Beijing summer conditions (T = 30 °C), $\varepsilon(NO_3^-)$ remains lower than 0.1, even until RH reaches 80%. When RH > 90%, $\varepsilon(NO_3^-)$ increases sharply as a function of RH. For T = 0 °C, representative of Beijing winter conditions, $\varepsilon(NO_3^-)$ is as high as 0.7, even at low RH. Figure 7 demonstrates the variations in the nitrate/sulfate ratio as a function of temperature and RH in Beijing. The nitrate/sulfate ratio increased with decreasing temperature and increasing RH, which drives the nitrate partitioning towards the particle phase. This is further supported by the variations in the equilibrium constant K_{AN} of Eq. (1), which can be calculated as:

$$K_{AN} = K_{AN}(298\ \mathrm{K})exp\left\{a\left(\frac{298}{T}-1\right)+b\left[1+ln\left(\frac{298}{T}\right)-\frac{298}{T}\right]\right\} \quad (3)$$

where T is the ambient temperature in Kelvin, K_{AN} (298) = 3.36 $\times 10^{16}$ (atm^{-2}), a = 75.11, and b = -13.5 (Seinfeld and Pandis, 2006). Similar to the nitrate/sulfate ratio, the diurnal profile of K_{AN} peaks at night due to the lower temperature and higher RH.

As described in Sect. 3.2, the rapid nitrate formation in this study appeared to be mainly associated with its nighttime enhancement. In addition to the effects of temperature and RH, the nighttime nitrate formation pathways may also play a role. Overnight, particulate nitrate primarily forms via the heterogeneous hydrolysis of N_2O_5 on the wet surface of aerosol (Ravishankara, 1997). N_2O_5 is produced by the reversible reaction between NO_2 and the NO_3 radical, where NO_2 reacts with O_3 to form the NO_3 radical. Assuming N_2O_5 and the NO_3 radical are both in steady state considering their short lifetimes (Brown et al., 2006), the nighttime production of N_2O_5 and HNO_3 is proportional to the concentration of NO_2 and O_3 ($[NO_2][O_3]$) (Young et al., 2016; Kim et al., 2017). For the different PM_1 concentration bins, we examined the NO_2 and O_3 data at 0:00 to assess the nighttime HNO_3 production rate. It can be seen that $[NO_2][O_3]$ was obviously enhanced with an increase in the PM_1 mass loading (Fig. S13), implying that nitrate formation by the N_2O_5 pathway favors the driving role of nitrate in haze evolution.

According to the Multi-resolution Emission Inventory for China (MEIC, http://www.meicmodel.org), NO_x emissions localized in Beijing are much smaller than emissions in adjacent Hebei, Shandong, and Henan provinces. In Fig. 1, episodes in Beijing, characterized by largely enhanced nitrate concentrations, usually occurred with the change in the wind direction from north and west to south and east, where the highly polluted Hebei, Shandong, and Henan provinces are located. When the relatively clean air masses from north and west returned, aerosol pollution was instantly swept away. Therefore, the importance of regional transport on haze formation in Beijing should also be considered. We examined the association of aerosol concentration and composition with air mass origins determined through cluster analysis of HYSPLIT back trajectories. As illustrated in Fig. 8, the aerosol characteristics are quite different for air masses from different regions. Cluster 1 mainly passed through Shanxi and Hebei provinces, and Cluster 2 originated from Hebei, Shandong, and Henan provinces. Consistent with the high air pollutant emissions in these areas, Cluster 1 and Cluster 2 were characterized with high PM_1 concentrations and high contributions of secondary aerosols. The nitrate fraction in PM_1 was 24% for Cluster 1 and 26% for Cluster 2. In comparison, Cluster 3 and Cluster 4 resulted from long-range transport from the cleaner northern areas and were correspondingly characterized by lower PM_1 concentrations. Organics dominated PM_1 for Cluster 3 and Cluster 4, with a nitrate contribution of 14% and 16%, respectively. Figure S14 shows the cluster distribution as a function of PM_1 concentration. With an increase in the PM_1 mass, the contribution of cleaner Cluster 3 and Cluster 4 significantly decreased. When PM_1 concentrations were above 20 μg m^{-3}, the air masses arriving in Beijing were mostly contributed by Cluster 1 and Cluster 2, which led to rapid nitrate accumulation.

3.4 Comparison with other regions and policy implications

Figure 9 summarizes the chemical composition of PM_1 or NR-PM_1 (BC excluded) measured during summer in Asia, Europe, and North America. Three types of sampling locations were included: urban areas, urban downwind areas, and rural/remote areas. Aerosol particles were dominated by organics (25.5-80.4%; avg = 48.1%) and secondary inorganic aerosols (18.0-73.7%; avg = 47.3%), and the nitrate contribution largely varied among different locations. Data for the pie charts are given in Table S3.

For further comparison, we classified the datasets into three groups according to the location type and examined their difference in nitrate mass concentrations and mass contributions. Overall, the nitrate concentrations varied from 0.04 μg m^{-3} to 17.6 μg m^{-3} in summer, with contributions of 0.9% to 25.2%. Patterns in Fig. 10 demonstrate that the nitrate concentrations in mainland China are usually much higher than those in other areas, consistent with the severe haze pollution in China. In particular, the percentage of nitrate in aerosol particles is generally several times higher in mainland China than in other regions, except for measurements in Riverside, CA, which were conducted near the local highway (Docherty et al., 2011). Compared to rural/remote areas, nitrate shows higher mass concentrations and mass fractions in urban and urban downwind areas, revealing the influence of anthropogenic emissions, i.e., traffic and power plant, on nitrate formation. In Beijing, the capital of China, field measurements among different years show an obvious reduction in the nitrate mass concentration, especially after 2011. The large decrease in nitrate concentration in the summer of 2008 was primarily caused by the strict emission control measures implemented during the 2008 Olympic Games (Wang et al., 2010). However, nitrate contributions in China still remain high over the years, especially in urban and urban downwind areas, revealing the importance of nitrate formation in haze episodes.

Due to the installation of flue-gas desulphurization (FGD) systems, the construction of larger units and the decommissioning of small units in power plants, SO_2 emissions in China decreased by 45% from 2005 to 2015 (Li et al., 2017d). However, NO_x emissions in China increased during the last decade. During the 11th Five-Year Plan (FYP), NO_x emissions showed a sustained and rapid growth with the economic development and the lack of relevant emissions controls. Since 2011, the government carried out end-of-pipe abatement strategies by installing selective catalytic reduction (SCR) in power plants and releasing strict emission regulations for vehicles. Based on the bottom-up emission inventory, NO_x emissions showed a decline of 21% from 2011 to 2015 (Liu et al., 2017). The changes are consistent with satellite-observed NO_2 levels in China (Miyazaki et al., 2017). Given the high concentration and, in particular, the high contribution of nitrate in aerosols, further NO_x reduction and initiation of NH_3 emission controls are in urgent need in China.

4 Conclusions

Summertime field measurements were conducted in both Beijing (30 June to 27 July, 2015) and Xinxiang (8 to 25 June, 2017) in the NCP region, using state-of-the-art online instruments to investigate the factors driving aerosol pollution. The average PM_1 concentration reached 35.0 μg m^{-3} in Beijing and 64.2 μg m^{-3} in Xinxiang, with significantly enhanced nitrate concentrations during pollution episodes. Secondary inorganic aerosol dominated PM_1, with high nitrate contributions of 24% in Beijing and 26% in Xinxiang. With the development of aerosol pollution, OA showed a decreasing contribution to total PM_1, despite its obvious domination at lower PM_1 mass loadings. The reduction in the OA mass fraction was primarily driven by primary sources (i.e., traffic and cooking emissions), especially in Beijing. Generally, the mass fraction of sulfate decreased slightly as a function of PM_1 concentration. In contrast, nitrate contribution enhanced rapidly and continuously with the elevation of PM_1 mass, suggesting the important role of nitrate formation in causing high aerosol pollution during summer. Rapid nitrate production mainly occurred after midnight, and the formation rate was higher for nitrate than for sulfate, SV-OOA, or LV-OOA.

Comprehensive analysis of nitrate behaviors revealed that abundant ammonia emissions in the NCP region favored the large nitrate formation in summer. According to the ISORROPIA-II thermodynamic predictions, $\varepsilon(NO_3^-)$ is significantly increased when there is more gas-phase ammonia in the atmosphere. Decreased SO_2 emissions have co-beneficial impacts on nitrate reduction. Lower temperature and higher RH drive the equilibrium partitioning of nitrate towards the particle phase, thus increasing the particulate nitrate concentration. As an indicator to evaluate the contribution of nighttime N_2O_5 hydrolysis to nitrate formation, $[NO_2][O_3]$ obviously enhanced at night with the anabatic pollution levels, suggesting the increased role of nighttime nitrate production in haze evolution. Based on cluster analysis via the HYSPLIT model, regional transport from surrounding polluted areas was found to play a role in increasing nitrate production during haze periods.

Finally, nitrate data acquired from this study were integrated with the literature results, including various field measurements conducted in Asia, Europe, and North America. Nitrate is present in higher mass concentrations and mass fractions in China than in other regions. Due to large anthropogenic emissions in urban and urban downwind areas, the mass concentrations and mass contributions of nitrate are much higher in these regions than in remote/rural areas. Although the nitrate mass concentrations in Beijing have steadily decreased over the years, its contribution still remains high, emphasizing the significance of further reducing NO_x emissions and NH_3 emissions in China.

Most of the previous studies conducted during wintertime reveal that secondary formation of sulfate together with primary emissions from coal combustion and biomass burning are important driving factors of haze evolution in the NCP region. According to this study, in Beijing and Xinxiang, rapid nitrate formation is regarded as the propulsion of aerosol pollution during summertime. Therefore, to better balance economic development and air pollution control, different emission control measures could be established corresponding to the specific driving forces of air pollution in different seasons. Further studies on seasonal variations are needed to test the conclusions presented here and provide more information on haze evolution in spring and fall.

Acknowledgements

This work was funded by the National Natural Science Foundation of China (41571130035, 41571130032 and 41625020).

References

Alexander, B., Hastings, M. G., Allman, D. J., Dachs, J., Thornton, J. A., and Kunasek, S. A.: Quantifying atmospheric nitrate formation pathways based on a global model of the oxygen isotopic composition (117O) of atmospheric nitrate, Atmos. Chem. Phys., 9, 5043–5056, doi:10.5194/acp-9-5043-2009, 2009.

Bougiatioti, A., Nikolaou, P., Stavroulas, I., Kouvarakis, G., Weber, R., Nenes, A., Kanakidou, M., and Mihalopoulos, N.: Particle water and pH in the eastern Mediterranean: source variability and implications for nutrient availability, Atmos Chem Phys, 16, 4579-4591, 10.5194/acp-16-4579-2016, 2016.

Brown, S. S., Ryerson, T. B., Wollny, A. G., Brock, C. A., Peltier, R., Sullivan, A. P., Weber, R. J., Dube, W. P., Trainer, M., Meagher, J. F., Fehsenfeld, F. C., and Ravishankara, A. R.: Variability in nocturnal nitrogen oxide processing and its role in regional air quality, Science, 311, 67-70, 10.1126/science.1120120, 2006.

Cheng, Y. F., Zheng, G. J., Wei, C., Mu, Q., Zheng, B., Wang, Z. B., Gao, M., Zhang, Q., He, K. B., Carmichael, G., Poschl, U., and Su, H.: Reactive nitrogen chemistry in aerosol water as a source of sulfate during haze events in China, Science Advances, 2, ARTN e1601530 10.1126/sciadv.1601530, 2016.

Cohen, A. J., Brauer, M., Burnett, R., Anderson, H. R., Frostad, J., Estep, K., Balakrishnan, K., Brunekreef, B., Dandona, L., Dandona, R., Feigin, V., Freedman, G., Hubbell, B., Jobling, A., Kan, H., Knibbs, L., Liu, Y., Martin, R., Morawska, L., Pope, C. A., Shin, H., Straif, K., Shaddick, G., Thomas, M., van Dingenen, R., van Donkelaar, A., Vos, T., Murray, C. J. L., and Forouzanfar, M. H.: Estimates and 25-year trends of the global burden of disease attributable to ambient air pollution: an analysis of data from the Global Burden of Diseases Study 2015, Lancet, 389, 1907-1918, 10.1016/S0140-6736(17)30505-6, 2017.

Docherty, K. S., Aiken, A. C., Huffman, J. A., Ulbrich, I. M., DeCarlo, P. F., Sueper, D., Worsnop, D. R., Snyder, D. C., Peltier, R. E., Weber, R. J., Grover, B. D., Eatough, D. J., Williams, B. J., Goldstein, A. H., Ziemann, P. J., and Jimenez, J. L.: The

2005 Study of Organic Aerosols at Riverside (SOAR-1): instrumental intercomparisons and fine particle composition, Atmos. Chem. Phys., 11, 12387-12420, https://doi.org/10.5194/acp-11-12387-2011, 2011.

Draxier, R. R., and Hess, G. D.: An overview of the HYSPLIT_4 modelling system for trajectories, dispersion and deposition, Aust Meteorol Mag, 47, 295-308, 1998.

Fountoukis, C. and Nenes, A.: ISORROPIA II: a computationally efficient thermodynamic equilibrium model for K^+–Ca^{2+}–Mg^{2+}–NH_4^+–Na^+–SO_4^{2-}–NO_3^-–Cl^-–H_2O aerosols, Atmos. Chem. Phys., 7, 4639-4659, https://doi.org/10.5194/acp-7-4639-2007, 2007.

Ge, X. L., He, Y. A., Sun, Y. L., Xu, J. Z., Wang, J. F., Shen, Y. F., and Chen, M. D.: Characteristics and Formation Mechanisms of Fine Particulate Nitrate in Typical Urban Areas in China, Atmosphere, 8, Artn 62 10.3390/Atmos8030062, 2017.

Guo, H., Xu, L., Bougiatioti, A., Cerully, K. M., Capps, S. L., Hite, J. R., Carlton, A. G., Lee, S. H., Bergin, M. H., Ng, N. L., Nenes, A., and Weber, R. J.: Fine-particle water and pH in the southeastern United States, Atmos Chem Phys, 15, 5211-5228, 10.5194/acp-15-5211-2015, 2015.

Guo, H., Sullivan, A. P., Campuzano-Jost, P., Schroder, J. C., Lopez-Hilfiker, F. D., Dibb, J. E., Jimenez, J. L., Thornton, J. A., Brown, S. S., Nenes, A., and Weber, R. J.: Fine particle pH and the partitioning of nitric acid during winter in the northeastern United States, J Geophys Res-Atmos, 121, 10355-10376, 10.1002/2016JD025311, 2016.

Guo, H. Y., Liu, J. M., Froyd, K. D., Roberts, J. M., Veres, P. R., Hayes, P. L., Jimenez, J. L., Nenes, A., and Weber, R. J.: Fine particle pH and gas-particle phase partitioning of inorganic species in Pasadena, California, during the 2010 CalNex campaign, Atmos Chem Phys, 17, 5703-5719, 10.5194/acp-17-5703-2017, 2017a.

Guo, H. Y., Weber, R. J., and Nenes, A.: High levels of ammonia do not raise fine particle pH sufficiently to yield nitrogen oxide-dominated sulfate production, Sci Rep-Uk, 7, Artn 12109 10.1038/S41598-017-11704-0, 2017b.

Guo, S., Hu, M., Zamora, M. L., Peng, J. F., Shang, D. J., Zheng, J., Du, Z. F., Wu, Z., Shao, M., Zeng, L. M., Molina, M. J., and Zhang, R. Y.: Elucidating severe urban haze formation in China, P Natl Acad Sci USA, 111, 17373-17378, 10.1073/pnas.1419604111, 2014.

Hennigan, C. J., Izumi, J., Sullivan, A. P., Weber, R. J., and Nenes, A.: A critical evaluation of proxy methods used to estimate the acidity of atmospheric particles, Atmos Chem Phys, 15, 2775-2790, 10.5194/acp-15-2775-2015, 2015.

Hu, W., Hu, M., Hu, W. W., Zheng, J., Chen, C., Wu, Y. S., and Guo, S.: Seasonal variations in high time-resolved chemical compositions, sources, and evolution of atmospheric submicron aerosols in the megacity Beijing, Atmos Chem Phys, 17, 9979-10000, 10.5194/acp-17-9979-2017, 2017.

Hu, W. W., Hu, M., Hu, W., Jimenez, J. L., Yuan, B., Chen, W. T., Wang, M., Wu, Y. S., Chen, C., Wang, Z. B., Peng, J. F., Zeng, L. M., and Shao, M.: Chemical composition, sources, and aging process of submicron aerosols in Beijing: Contrast between summer and winter, J Geophys Res-Atmos, 121, 1955-1977, 10.1002/2015JD024020, 2016.

Huang, R. J., Zhang, Y. L., Bozzetti, C., Ho, K. F., Cao, J. J., Han, Y. M., Daellenbach, K. R., Slowik, J. G., Platt, S. M., Canonaco, F., Zotter, P., Wolf, R., Pieber, S. M., Bruns, E. A., Crippa, M., Ciarelli, G., Piazzalunga, A., Schwikowski, M., Abbaszade, G., Schnelle-Kreis, J., Zimmermann, R., An, Z. S., Szidat, S., Baltensperger, U., El Haddad, I., and Prevot, A. S. H.: High secondary aerosol contribution to particulate pollution during haze events in China, Nature, 514, 218-222, 10.1038/nature13774, 2014.

IPCC: Summary for Policymakers, in: Climate Change 2007: The Physical Science Basis. Contribution of Working Group I to the Fourth Assessment Report of the Intergovernmental Panel on Climate Change, edited by: Solomon, S., Qin, D., Manning, M., Chen, Z., Marquis, M., Averyt, K. B., M.Tignor, and Miller, H. L., Cambridge University Press, Cambridge, UK and New York, NY, USA, 1–18, 2007.

Jimenez, J. L., Canagaratna, M. R., Donahue, N. M., Prevot, A. S. H., Zhang, Q., Kroll, J. H., DeCarlo, P. F., Allan, J. D., Coe, H., Ng, N. L., Aiken, A. C., Docherty, K. S., Ulbrich, I. M., Grieshop, A. P., Robinson, A. L., Duplissy, J., Smith, J. D., Wilson, K. R., Lanz, V. A., Hueglin, C., Sun, Y. L., Tian, J., Laaksonen, A., Raatikainen, T., Rautiainen, J., Vaattovaara, P., Ehn, M., Kulmala, M., Tomlinson, J. M., Collins, D. R., Cubison, M. J., Dunlea, E. J., Huffman, J. A., Onasch, T. B., Alfarra, M. R., Williams, P. I., Bower, K., Kondo, Y., Schneider, J., Drewnick, F., Borrmann, S., Weimer, S., Demerjian, K., Salcedo, D., Cottrell, L., Griffin, R., Takami, A., Miyoshi, T., Hatakeyama, S., Shimono, A., Sun, J. Y., Zhang, Y. M., Dzepina, K., Kimmel, J. R., Sueper, D., Jayne, J. T., Herndon, S. C., Trimborn, A. M., Williams, L. R., Wood, E. C., Middlebrook, A. M., Kolb, C. E., Baltensperger, U., and Worsnop, D. R.: Evolution of Organic Aerosols in the Atmosphere, Science, 326, 1525-1529, 10.1126/science.1180353, 2009.

Kim, H., Zhang, Q., and Heo, J.: Influence of Intense secondary aerosol formation and long range transport on aerosol chemistry and properties in the Seoul Metropolitan Area during spring time: Results from KORUS-AQ, Atmos. Chem. Phys. Discuss., https://doi.org/10.5194/acp-2017-947, in review, 2017.

Kouimtzis, T., and Samara, C.: Airborne Particulate Matter, Springer, 1995.

Li, H., Zhang, Q., Duan, F., Zheng, B., and He, K.: The “Parade Blue”: effects of short-term emission control on aerosol chemistry, Faraday Discuss., 189, 317–335, 2016.

Li, Y. J., Sun, Y., Zhang, Q., Li, X., Li, M., Zhou, Z., and Chan, C. K.: Real-time chemical characterization of atmospheric particulate matter in China: A review, Atmos Environ, 158, 270-304, https://doi.org/10.1016/j.atmosenv.2017.02.027, 2017a.

Li, H. Y., Zhang, Q., Zhang, Q., Chen, C. R., Wang, L. T., Wei, Z., Zhou, S., Parworth, C., Zheng, B., Canonaco, F., Prevot, A. S. H., Chen, P., Zhang, H. L., Wallington, T. J., and He, K. B.: Wintertime aerosol chemistry and haze evolution in an extremely

polluted city of the North China Plain: significant contribution from coal and biomass combustion, Atmos Chem Phys, 17, 4751-4768, 10.5194/acp-17-4751-2017, 2017b.

Li, C., McLinden, C., Fioletov, V., Krotkov, N., Carn, S., Joiner, J., Streets, D., He, H., Ren, X. R., Li, Z. Q., and Dickerson, R. R.: India Is Overtaking China as the World's Largest Emitter of Anthropogenic Sulfur Dioxide, Sci Rep-Uk, 7, Artn 14304 10.1038/S41598-017-14639-8, 2017c.

Li, M., Liu, H., Geng, G. N., Hong, C. P., Liu, F., Song, Y., Tong, D., Zheng, B., Cui, H. Y., Man, H. Y., Zhang, Q., and He, K. B.: Anthropogenic emission inventories in China: a review, Natl Sci Rev, 4, 834-866, 10.1093/nsr/nwx150, 2017d.

Liu, F., Beirle, S., Zhang, Q., van der A, R. J., Zheng, B., Tong, D., and He, K. B.: NO_x emission trends over Chinese cities estimated from OMI observations during 2005 to 2015, Atmos Chem Phys, 17, 9261-9275, 10.5194/acp-17-9261-2017, 2017.

Liu, M., Song, Y., Zhou, T., Xu, Z., Yan, C., Zheng, M., Wu, Z., Hu, M., Wu, Y., and Zhu, T.: Fine particle pH during severe haze episodes in northern China, Geophys Res Lett, 44, 2017GL073210, 10.1002/2017GL073210, 2017.

Miyazaki, K., Eskes, H., Sudo, K., Boersma, K. F., Bowman, K., and Kanaya, Y.: Decadal changes in global surface NO_x emissions from multi-constituent satellite data assimilation, Atmos. Chem. Phys., 17, 807-837, https://doi.org/10.5194/acp-17-807-2017, 2017.

Ng, N. L., Herndon, S. C., Trimborn, A., Canagaratna, M. R., Croteau, P. L., Onasch, T. B., Sueper, D., Worsnop, D. R., Zhang, Q., Sun, Y. L., and Jayne, J. T.: An Aerosol Chemical Speciation Monitor (ACSM) for Routine Monitoring of the Composition and Mass Concentrations of Ambient Aerosol, Aerosol Sci Tech, 45, 780-794, Pii 934555189 10.1080/02786826.2011.560211, 2011.

Paatero, P., and Tapper, U.: Positive Matrix Factorization - a Nonnegative Factor Model with Optimal Utilization of Error-Estimates of Data Values, Environmetrics, 5, 111-126, DOI 10.1002/env.3170050203, 1994.

Pathak, R. K., Wang, T., and Wu, W. S.: Nighttime enhancement of PM2.5 nitrate in ammonia-poor atmospheric conditions in Beijing and Shanghai: Plausible contributions of heterogeneous hydrolysis of N2O5 and HNO3 partitioning, Atmos Environ, 45, 1183-1191, 10.1016/j.atmosenv.2010.09.003, 2011.

Petzold, A. and Schonlinner, M.: Multi-angle absorption photometry – a new method for the measurement of aerosol light absorption and atmospheric black carbon, J. Aerosol Sci., 35, 421–441, 2004.

Petzold, A., Schloesser, H., Sheridan, P. J., Arnott, W. P., Ogren, J. A., and Virkkula, A.: Evaluation of multiangle absorption photometry for measuring aerosol light absorption, Aerosol Sci. Tech., 39, 40–51, 2005.

Pope, C. A., Ezzati, M., and Dockery, D. W.: Fine-Particulate Air Pollution and Life Expectancy in the United States, New England Journal of Medicine, 360, 376–386, doi:10.1056/NEJMsa0805646, 2009.

Ravishankara, A. R.: Heterogeneous and multiphase chemistry in the troposphere, Science, 276, 1058-1065, DOI 10.1126/science.276.5315.1058, 1997.

Seinfeld, J. H. and Pandis, S. N.: Atmospheric Chemistry and Physics: From Air Pollution to Climate Change, John Wiley & Sons, New York, 2nd edition, 1232 pp., ISBN-13: 978-0-471-72018-8, 2006.

Sun, Y. L., Wang, Z. F., Dong, H. B., Yang, T., Li, J., Pan, X. L., Chen, P., and Jayne, J. T.: Characterization of summer organic and inorganic aerosols in Beijing, China with an Aerosol Chemical Speciation Monitor, Atmos Environ, 51, 250-259, 10.1016/j.atmosenv.2012.01.013, 2012.

Sun, Y. L., Wang, Z. F., Dong, H. B., Yang, T., Li, J., Pan, X. L., Chen, P., and Jayne, J. T.: Characterization of summer organic and inorganic aerosols in Beijing, China with an Aerosol Chemical Speciation Monitor, Atmos Environ, 51, 250-259, 10.1016/j.atmosenv.2012.01.013, 2012.Sun, Y. L., Wang, Z. F., Du, W., Zhang, Q., Wang, Q. Q., Fu, P. Q., Pan, X. L., Li, J., Jayne, J., and Worsnop, D. R.: Long-term real-time measurements of aerosol particle composition in Beijing, China: seasonal variations, meteorological effects, and source analysis, Atmos Chem Phys, 15, 10149-10165, 10.5194/acp-15-10149-2015, 2015.

Sun, J. X., Liu, L., Xu, L., Wang, Y. Y., Wu, Z. J., Hu, M., Shi, Z. B., Li, Y. J., Zhang, X. Y., Chen, J. M., and Li, W. J.: Key Role of Nitrate in Phase Transitions of Urban Particles: Implications of Important Reactive Surfaces for Secondary Aerosol Formation, J Geophys Res-Atmos, 123, 1234-1243, 10.1002/2017JD027264, 2018.

Ulbrich, I. M., Canagaratna, M. R., Zhang, Q., Worsnop, D. R., and Jimenez, J. L.: Interpretation of organic components from Positive Matrix Factorization of aerosol mass spectrometric data, Atmos Chem Phys, 9, 2891-2918, 10.5194/acp-9-2891-2009, 2009.

Watson, J. G.: Visibility: Science and regulation, J. Air Waste Manage. Assoc., 52, 628–713, doi:10.1080/10473289.2002.10470813, 2002.

Wang, H., Lu, K., Chen, X., Zhu, Q., Chen, Q., Guo, S., Jiang, M., Li, X., Shang, D., Tan, Z., Wu, Y., Wu, Z., Zou, Q., Zheng, Y., Zeng, L., Zhu, T., Hu, M., and Zhang, Y.: High N2O5 Concentrations Observed in Urban Beijing: Implications of a Large Nitrate Formation Pathway, Environ Sci Tech Let, 10.1021/acs.estlett.7b00341, 2017.

Wang, S. X., Zhao, M., Xing, J., Wu, Y., Zhou, Y., Lei, Y., He, K. B., Fu, L. X., and Hao, J. M.: Quantifying the Air Pollutants Emission Reduction during the 2008 Olympic Games in Beijing, Environ Sci Technol, 44, 2490-2496, 10.1021/es9028167, 2010.

Weber, R. J., Guo, H. Y., Russell, A. G., and Nenes, A.: High aerosol acidity despite declining atmospheric sulfate concentrations over the past 15 years, Nat Geosci, 9, 282-+, 10.1038/NGEO2665, 2016.

Yang, T., Sun, Y., Zhang, W., Wang, Z., Liu, X., Fu, P., and Wang, X.: Evolutionary processes and sources of high-nitrate haze episodes over Beijing, Spring, J Environ Sci-China, 54, 142-151, http://dx.doi.org/10.1016/j.jes.2016.04.024, 2017.

Young, D. E., Kim, H., Parworth, C., Zhou, S., Zhang, X. L., Cappa, C. D., Seco, R., Kim, S., and Zhang, Q.: Influences of emission sources and meteorology on aerosol chemistry in a polluted urban environment: results from DISCOVER-AQ California, Atmos Chem Phys, 16, 5427-5451, 10.5194/acp-16-5427-2016, 2016.

Zhang, Q., Jimenez, J. L., Canagaratna, M. R., Ulbrich, I. M., Ng, N. L., Worsnop, D. R., and Sun, Y.: Understanding atmospheric organic aerosols via factor analysis of aerosol mass spectrometry: a review, Anal. Bioanal. Chem., 401, 3045–3067, 2011.

Zhang, Q., He, K. B., and Huo, H.: Cleaning China's air, Nature, 484, 161-162, 2012.

Zheng, B., Zhang, Q., Zhang, Y., He, K. B., Wang, K., Zheng, G. J., Duan, F. K., Ma, Y. L., and Kimoto, T.: Heterogeneous chemistry: a mechanism missing in current models to explain secondary inorganic aerosol formation during the January 2013 haze episode in North China, Atmos Chem Phys, 15, 2031-2049, 10.5194/acp-15-2031-2015, 2015.

Zou, Y., Wang, Y., Zhang, Y., and Koo, J.-H.: Arctic sea ice, Eurasia snow, and extreme winter haze in China, Science Advances, 3, 10.1126/sciadv.1602751, 2017.

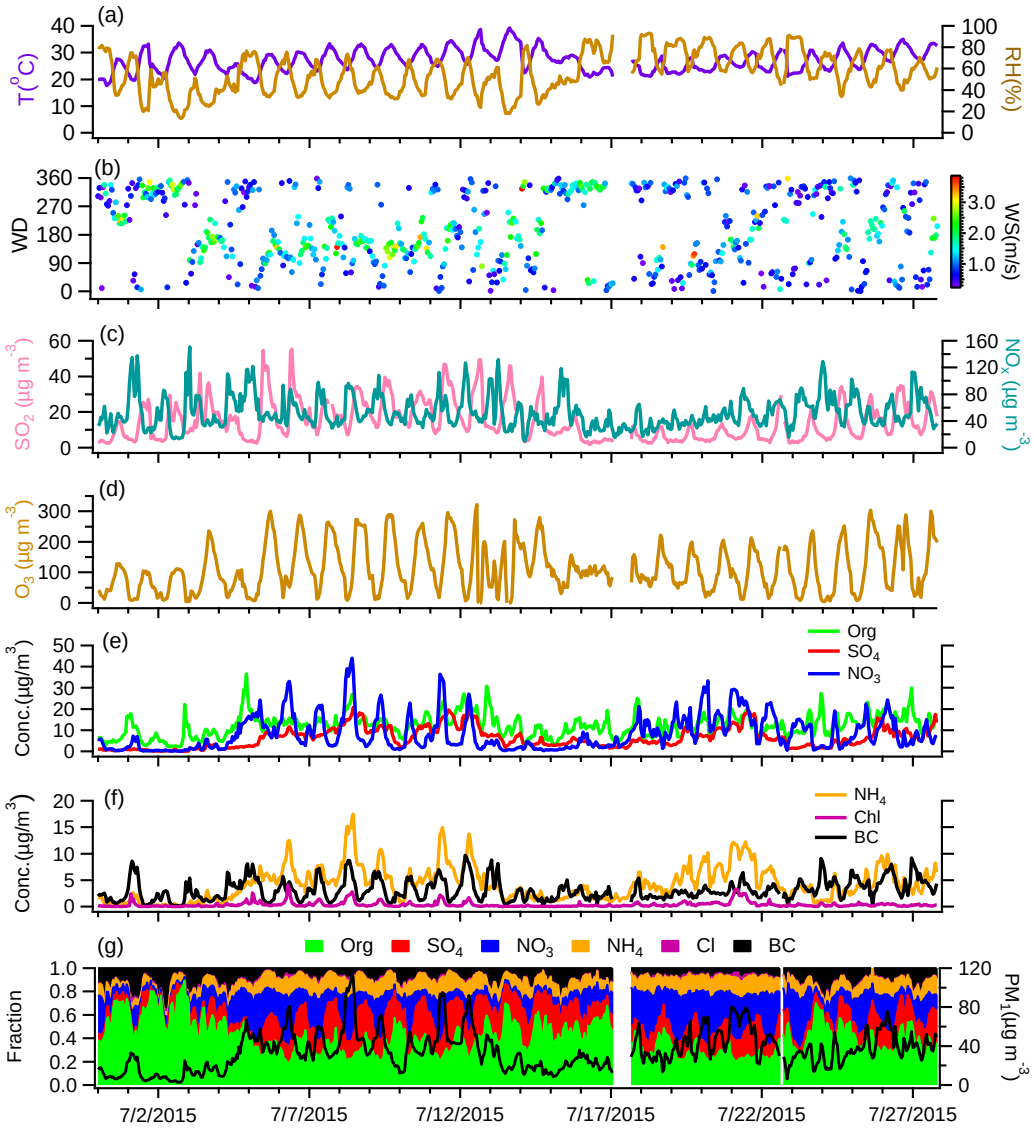

Figure 1. Time series of meteorological parameters, gaseous species, and submicron aerosol species in Beijing.

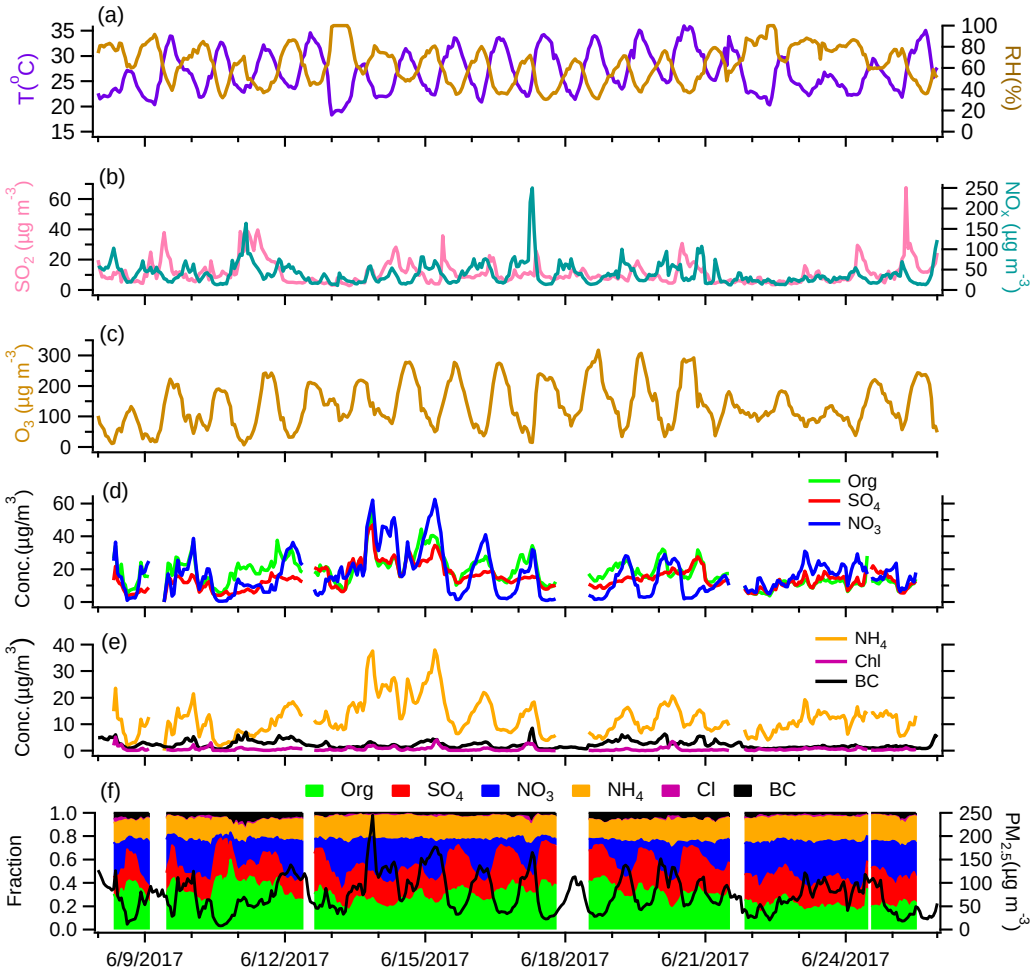

Figure 2. Time series of meteorological parameters, gaseous species, and submicron aerosol species in Xinxiang.

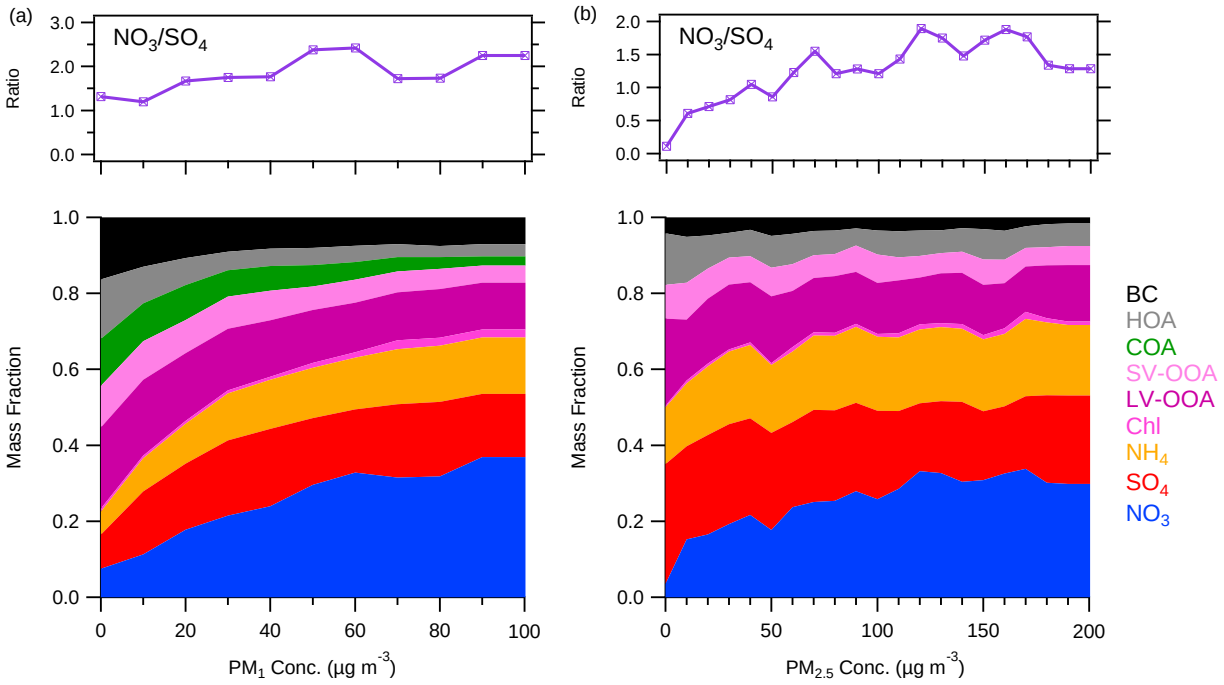

Figure 3. Variations in the mass fraction of aerosol species and nitrate/sulfate mass ratio as a function of total PM_1 mass loadings in (a) Beijing and (b) Xinxiang.

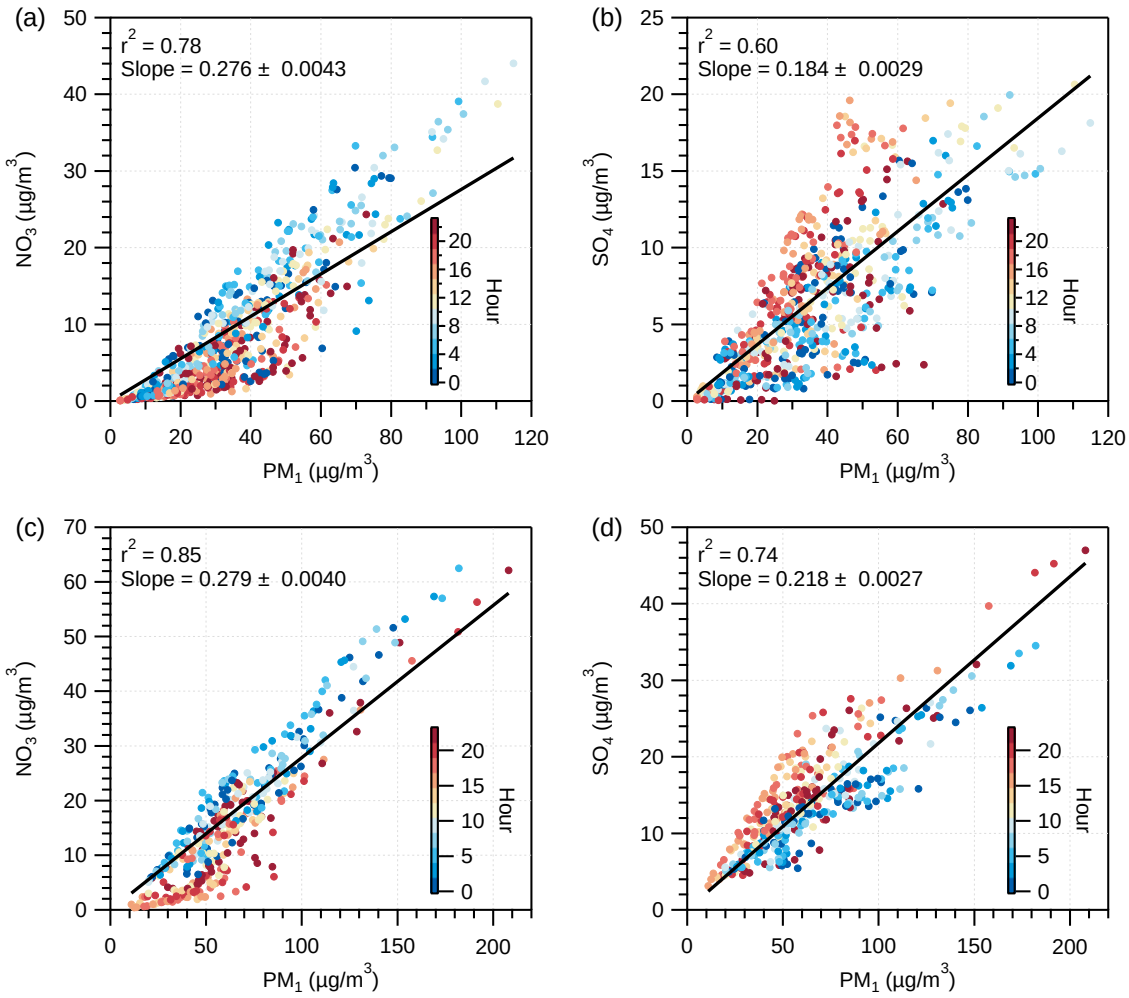

Figure 4. Scatterplots of nitrate vs. PM_1 concentration and sulfate vs. PM_1 concentration, colored by the hour of the day, in (a-b) Beijing and (c-d) Xinxiang.

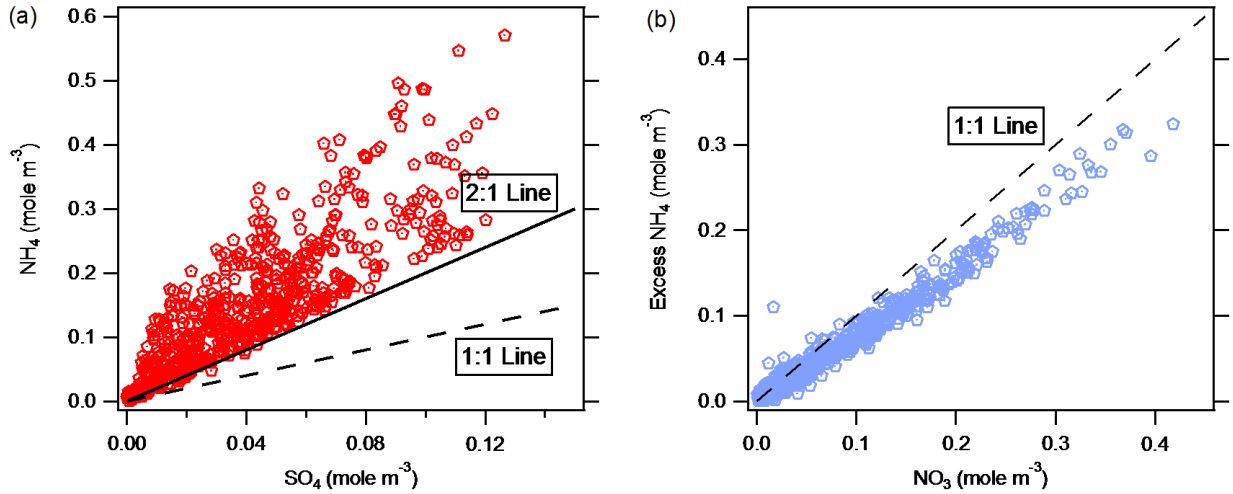

Figure 5. Comparison of the molar concentrations of (a) ammonium and sulfate (the 2:1 reference line represents complete H_2SO_4 neutralization) and (b) excess ammonium and nitrate (the 1:1 reference line represents complete HNO3 neutralization).

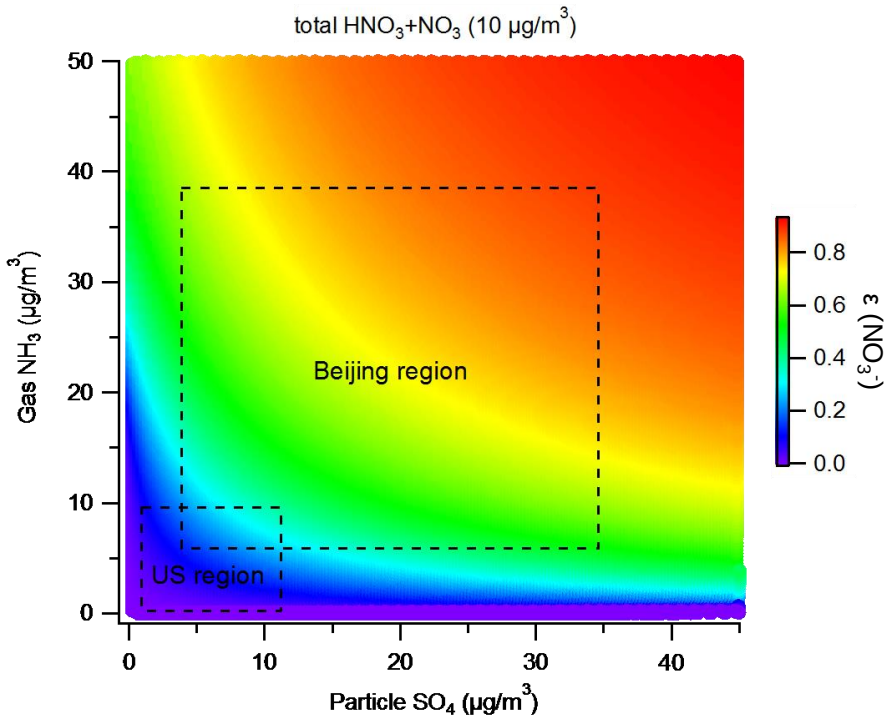

Figure 6. Sensitivity of the nitrate partitioning ratio ($\varepsilon(NO_3^-) = NO_3^-/(HNO_3 + NO_3^-)$) to gas-phase ammonia and PM_1 sulfate concentrations based on thermodynamic predictions under typical Beijing and Xinxiang summertime conditions. The total nitrate concentration is assumed to be 10 μg m^{-3}, according to the observed PM_1 nitrate concentration.

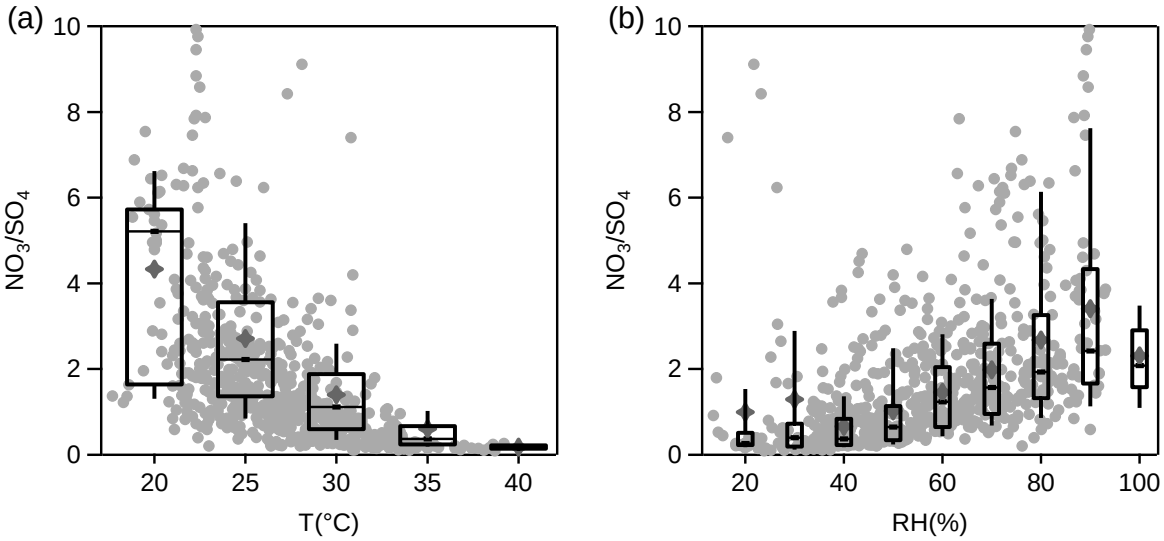

Figure 7. Variations in the nitrate/sulfate mass ratio as a function of (a) temperature (T) and (b) relative humidity (RH). The data were binned according to T and RH, and the mean (cross), median (horizontal line), 25th and 75th percentiles (lower and upper box), and 10th and 90th percentiles (lower and upper whiskers) are shown for each bin.

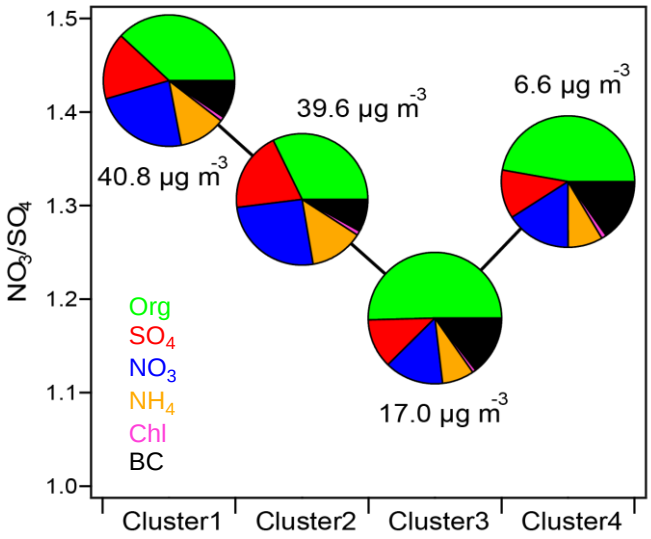

Figure 8. Nitrate/sulfate mass ratios for each cluster. The pie charts represent the average PM_1 chemical composition of the different clusters. In addition, the total PM_1 concentrations for each cluster are also shown.

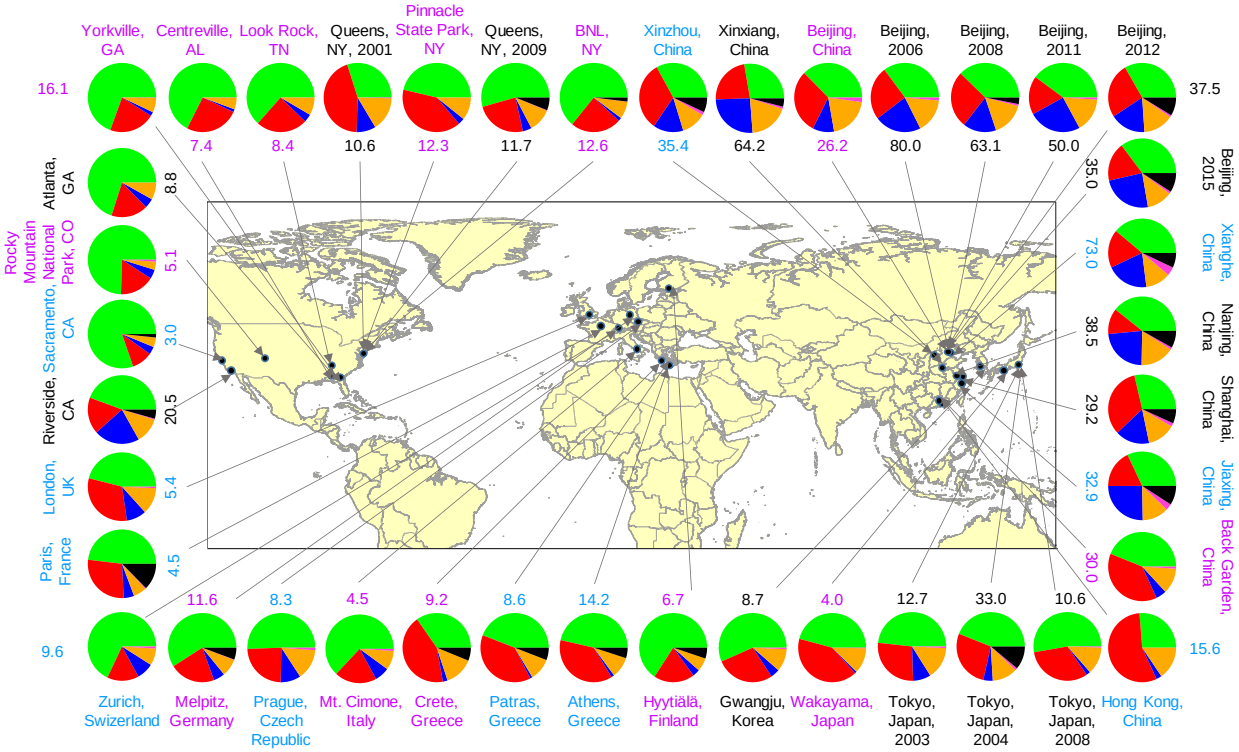

Figure 9. Summary of the submicron particle measurements using ACSM or Aerosol Mass Spectrometer in Asia, Europe, and North America (data given in Table S1 in the supplementary materials). Colors for the study labels indicate the type of sampling location: urban areas (black), urban downwind areas (blue), and rural/remote areas (pink). The pie charts show the average mass concentration and chemical composition of PM_1 or NR-PM_1: organics (green), sulfate (red), nitrate (blue), ammonium (orange), chloride (purple), and BC (black).

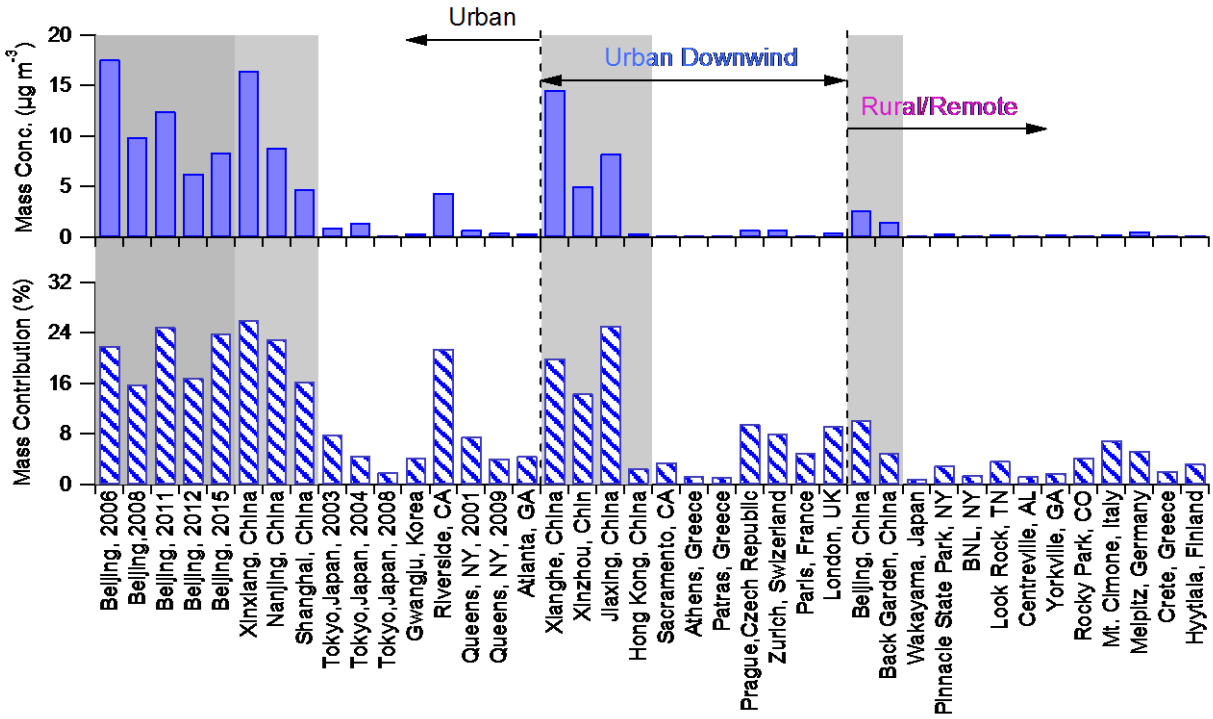

Figure 10. Average mass concentrations and mass fractions of nitrate at various sampling sites for three types of locations: urban, urban downwind, and rural/remote areas. Within each category, the sites are ordered from left to right as Asia, North America, and Europe. The shaded area indicates the results from China.